

# We are IntechOpen, the world's leading publisher of Open Access books Built by scientists, for scientists

6,900

Open access books available

185,000

International authors and editors

200M

Downloads

Our authors are among the

154

Countries delivered to

TOP 1%

most cited scientists

12.2%

Contributors from top 500 universities



WEB OF SCIENCE™

Selection of our books indexed in the Book Citation Index  
in Web of Science™ Core Collection (BKCI)

Interested in publishing with us?  
Contact [book.department@intechopen.com](mailto:book.department@intechopen.com)

Numbers displayed above are based on latest data collected.  
For more information visit [www.intechopen.com](http://www.intechopen.com)



# Anomalous Diffusivity in Porous Solids: Levitation Effect

*Shubhadeep Nag and Yashonath Subramanian*

## Abstract

Fluids confined to zeolites and other porous solids exhibit many distinct properties. One such property is the diffusivity, which exhibits anomalous dependence on the size of the guest molecule confined to the pore. This is termed the levitation effect. A diffusivity maximum as a function of the diameter of the guest is seen. The diameter for which the guest has maximum diffusivity is seen to be associated with a minimum in the activation energy. The existence of similar behavior in other porous solids, framework flexibility, and effect of temperature are discussed. Experimental verification of the existence of the anomalous maximum is then discussed. Diffusion of *n*-hexane and its isomers in zeolite NaY are then discussed in detail. The reduction in the end-to-end length of *n*-hexane while passing through the 12-ring window and the reasons for the same are discussed. Section 3 discusses possible observations of size-dependent maximum in other condensed matter systems.

**Keywords:** diffusivity, zeolites, porous solids, anomalous diffusivity, size dependence

## 1. Introduction

Zeolites are excellent catalysts due to the presence of acid sites on the framework. These catalyze a number of reactions such as hydrocarbon isomerization, hydrocarbon cracking or transformation. In recent times, there have been considerable increase in investigations pertaining to various aspects of zeolites [1–13]. There have been several studies aimed at clarifying the mechanism involved in the reactions catalyzed by zeolites. Boronat and Corma have discussed the changes in energy on proton exchange between zeolite and an adsorbate. They attempt to compute the contribution due to the van der Waals interaction between the zeolite and the adsorbate, which can be significant when the molecules are of size similar to the pore [1]. Davis and coworkers have attempted synthesis of enantiomerically enriched molecular sieve. Recently they succeeded in such a synthesis and this has been discussed in a recent article [11, 13]. Corma and coworkers have discussed various novel approaches to the synthesis of zeolites [3]. Dusselier and Davis have discussed at length the synthesis and the use in catalysis of small pore zeolites [12]. Corma and coworkers have discussed the synthesis of a new all-silica polymorph ITQ-55, which is highly efficient in the separation of ethane and ethylene with a high selectivity of 100 [4]. Prashant Kumar et al. [9] have pointed out the novel synthesis of MFI nanosheets with sandwiched MEL. Zeolite can be used for separation of xylene isomers with a high degree of separation [8]. From these it is evident

that many new and novel aspects of zeolites are still being discovered and zeolites continues to be an exciting field of research with a bounty of surprises.

Zeolites are porous aluminosilicates capable of accommodating molecules within the pores. They are well known for their catalytic, ion-exchange, and separation properties. They are widely used in petrochemical industries for processing hydrocarbons. Hydrocarbon cracking, transformation, isomerization, etc. are achieved with the help of zeolites [14, 15]. Zeolites are also used in separating hydrocarbon molecules of various sizes [16]. Larger hydrocarbons such as C15 and with still higher number of carbon atoms diffuse slowly through the pores and hence reach the bottom of a zeolite column last. Small molecules such as C1-C5 diffuse fast and exit from the column first [17, 18]. Other molecules of intermediate size have values of diffusivity in between those of C15 and C1-C5 and exit at intermediate times. Thus the various fractions from crude can be separated. This separation is much more energy efficient as compared to separation by distillation.

Another application of zeolites is its use for ion-exchange and water softening [19, 20]. Ions such as  $\text{Ca}^{2+}$  can be exchanged with  $\text{Na}^+$  already present in the zeolites, thus removing these ions from water. Zeolites are therefore used in detergents for washing clothes.

Apart from the use of zeolite for separation based on the size of the molecule, it is also of considerable use for separations based on the shape of the molecules. This property of zeolites is often referred to as shape selectivity [21]. The pore dimensions of zeolites, which are not always of regular shape, make this possible. An oft quoted example is the separation of xylenes (p-, m-, and o-xylenes) using silicate or ZSM-5 [22, 23]. At sufficiently high temperatures, o-xylene will convert to p-xylene and ZSM-5 also acts as a catalyst.

Zeolites and other host materials also exhibit interesting properties. They exhibit window effect, single file diffusion, and levitation effect [24–26]. Here we will focus on the levitation effect, which refers to the dependence of diffusivity on the guest or diffusant diameter.

## **2. Diffusivity of guest molecules confined to the pores from MD simulations**

In order to understand the diffusion of hydrocarbon and other molecules within the confined spaces of the zeolite, it is essential to carry out an investigation into diffusivity of guest molecules within the confined space provided by a zeolite or other porous solids. Such a study is essential for an understanding of the process of separation of hydrocarbon as well as other mixtures.

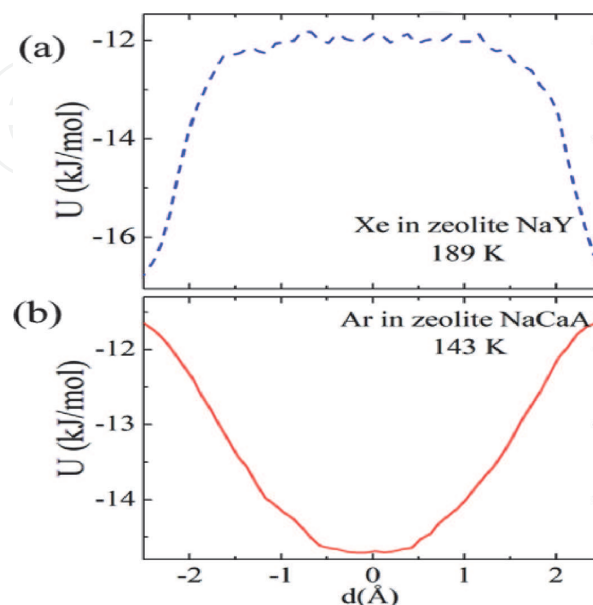
One of the early studies investigating the diffusivity of guest molecules in zeolites was the diffusion of xenon in zeolite Y and argon in NaCaA [27]. The diffusivity is likely to be strongly influenced by the bottleneck for diffusion. In the case of xenon the bottleneck is the 12-ring window, which has a diameter of around 7.8 Å. In the case of argon the bottleneck is an 8-ring window, which has a diameter of around 4.5 Å. The ratio of the bottleneck to the molecular/atomic diameter for xenon-NaY system is  $7.0/4.1 = 1.70$  while in the case of argon-NaCaA it is  $4.0/3.405 = 1.17$ . Although the diameters of the windows are approximate, it is clear that the window diameter is significantly larger than the diameter of xenon while this is not true for argon where the diameter of the window is only slightly larger than the argon diameter. From these it is evident that xenon in NaY should have a higher diffusivity than argon in NaCaA.

From MD, it was found that xenon in NaY has a diffusivity of  $0.19 \times 10^{-8} \text{ m}^2/\text{s}$  while argon in NaCaA has a diffusivity of  $0.9 \times 10^{-8} \text{ m}^2/\text{s}$ . As the diffusivity of

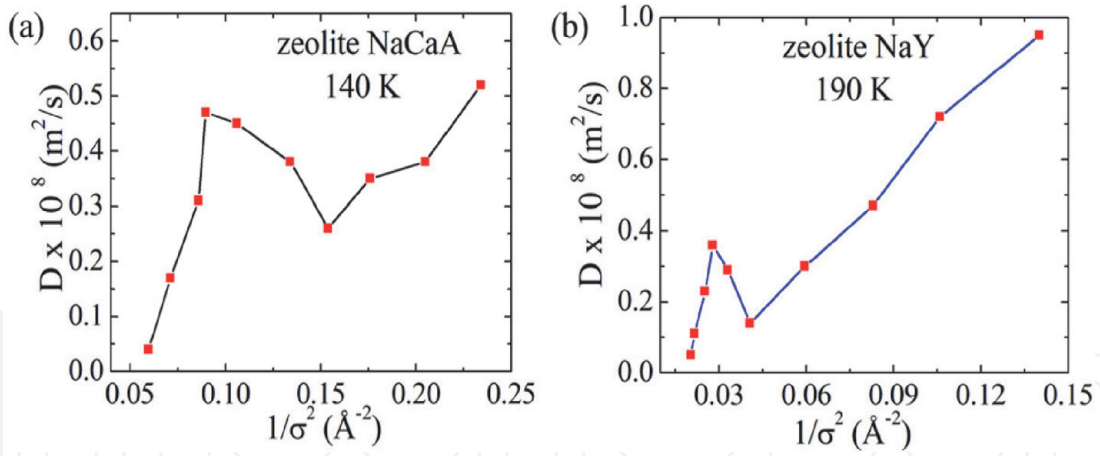
argon in NaCaA is higher than xenon in NaY, further investigations were carried out to find the reasons for this. To start with the energy barrier at the bottleneck was computed. This is shown in **Figure 1** [27]. From the figure it is seen that the energy barrier for xenon at the window in Y is positive while the barrier at the window is negative for argon in A zeolite. This explains why the diffusivity of argon in A zeolite is higher than xenon in Y zeolite. The trends seen in the observed barrier appears to be due to the strong interaction of argon with the oxygens of the 8-ring window. As argon is about the same diameter as the window, its strength of interaction with the oxygens is optimum being close to  $\epsilon$ , which occurs at a distance at which the Lennard-Jones curve is minimum in energy. This is not the case for xenon in zeolite Y where xenon can be close to only some of the oxygens of the 12-ring window. This is the first indication that nongeometrical factors can influence the diffusivity. This study shows that sorbate-zeolite interaction plays an important role.

This study suggests that an understanding of diffusivity as a function of the diameter of the guest species might show something interesting. Such a study was carried out and the results were indeed found to be interesting [28]. A molecular dynamics study of monatomic guest molecules confined to zeolite NaY and NaCaA were carried out in which the diameter of the guest molecule was varied. The diffusivities of the guest species was computed from the time evolution of the mean square displacements. A plot of diffusivity as a function of the reciprocal of square of the guest diameter is shown in **Figure 2** for guests in both zeolites Y and A [28]. It is seen that the diffusivities decrease linearly with increase in the reciprocal of the square of the diameter of the guest molecule for small diameters. This is referred to as the linear regime (LR). As the diameter increases, it is seen that the diffusivity suddenly increases and later decreases sharply exhibiting a maximum in diffusivity. This is referred to as the anomalous regime (AR). This increase followed by a decrease in diffusivity was surprising and needed further investigations.

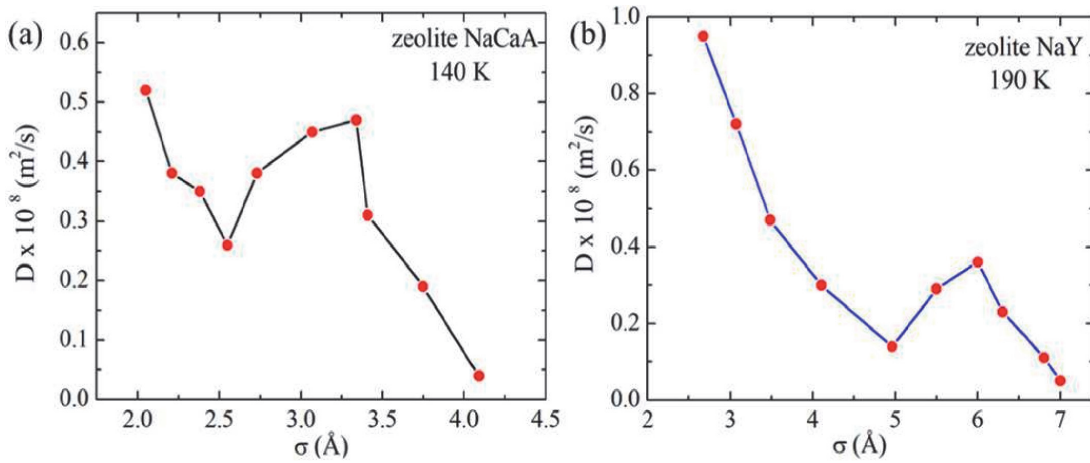
As can be seen the location of the guest diameter at which the maximum occurs is different in both zeolite Y and A (see **Figure 3** [28]). In order to understand the reasons for the maximum in diffusivity we have tried to search in literature any report that refers to such an observation. Derouane and coworkers have reported a finding arrived at through a theoretical analysis. They showed that the nesting



**Figure 1.** Potential energy landscape of (a) xenon in zeolite NaY at 190 K and (b) argon in zeolite NaCaA at 140 K. the energy landscapes are computed from molecular dynamics simulations.


**Figure 2.**

Diffusion coefficient of guest particles is plotted as a function of  $1/\sigma^2$ , where  $\sigma$  is the guest diameter.  $D$  for guest confined to (a) zeolite NaCaA at 140 K and to (b) zeolite NaY at 190 K temperature, where  $1/\sigma^2$  is the inverse square of the vdw radius of guest particles.


**Figure 3.**

Diffusion coefficient,  $D$  as a function of vdw radius of guest particles,  $\sigma$  is plotted in (a) zeolite NaCaA at 140 K and in (b) zeolite NaY at 190 K temperature.

effect can lead to *floating molecules* when the pore diameter is comparable to the molecular diameter. Earlier Kemball found that when guest molecules are sorbed inside host materials such as zeolites or other adsorbents it is seen that some undergo little loss of entropy. In such systems, he suggested, the guest molecules will exhibit high mobility or *superdiffusivity*.

In order to obtain a better understanding, we define a dimensionless parameter

$$\gamma = \frac{2 \times 2^{1/6} \sigma_{gz}}{\sigma_w} \quad (1)$$

where the numerator gives the distance at which the interactions between the guest and the zeolite atoms are optimum, that is, when this gives an interaction energy of  $\epsilon_{gz}$ . The denominator is the window radius. Thus, the dimensionless parameter suggests that when these two are equal ( $\gamma = 1$ ) and when they are not equal ( $\gamma \ll 1$ ). We now plot the diffusivity as a function of  $\gamma$ . This is shown in **Figure 4** [28]. We see that the maximum is seen when  $\gamma$  is between 0.9 and 1.0 for *both* the zeolites. Thus, the guest-zeolite interaction is optimum at  $2^{1/6} \sigma_{gz}$  and when this equals  $\sigma_w/2$ , the diffusivity maximum is seen. This situation when  $\gamma$  is close to unity is illustrated in **Figure 5** along with the situation when  $\gamma \ll 1$ . Now when  $\gamma$  is close to unity the guest molecule is passing through the center of the window. Such a position has inversion symmetry, which leads to mutual cancelation of forces

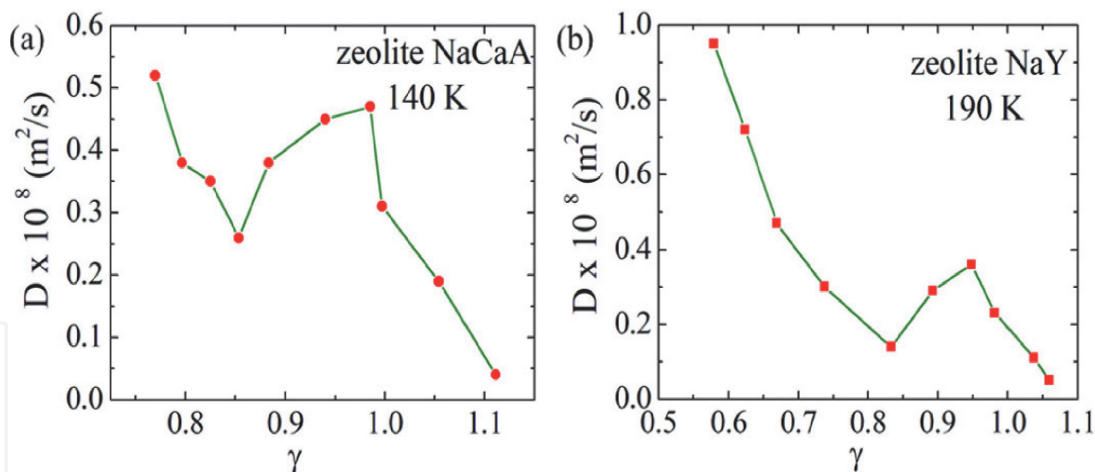


**Figure 4.** Diffusion coefficient,  $D$  is plotted as a function of levitation parameter,  $\gamma$  (see text) in (a) zeolite NaCaA at 140 K and in (b) zeolite NaY at 190 K temperature.

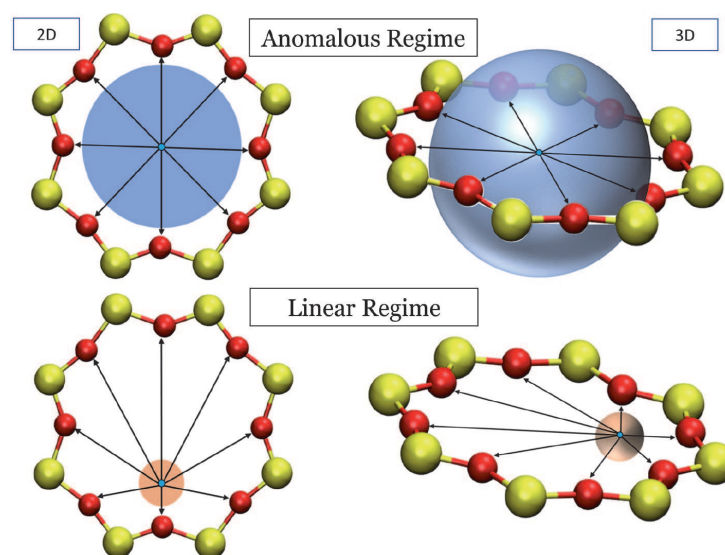


**Figure 5.** Schematic figure indicating the position of bigger and smaller particles while passing through the zeolite window. It is shown that the bigger particle passes through the symmetry position, the center of the window, whereas the smaller particle is near to the periphery of the window. Therefore, the forces along a given direction is equal and opposite to that exerted on the bigger particle from the diagonally opposite direction, resulting in higher diffusion than for the smaller particle, which is attracted to the periphery, and therefore experiences a net attraction. This is shown in both 2D and 3D.

leading to rather small force on the guest due to the zeolite. This situation is akin to the guest being a free particle even when confined within the zeolite and therefore has a high diffusivity.

When  $\gamma \ll 1$  the guest passes through the window at the periphery. These points do not possess inversion symmetry and therefore there is no cancellation of forces exerted on the guest by the zeolite. This leads to lower diffusivity of these guest molecules.

The reason for the observed maximum in diffusivity arises from the lowered force on the guest molecule as compared to the smaller guest molecule, which encounters a higher force on itself due to the zeolite. These translate to a less undulating potential energy landscape with shallower minima and maxima for the larger guest molecule for which  $\gamma$  is close to unity. In the case of smaller guest molecule the larger force implies a highly undulating potential energy landscape with deep valleys and high mountains. However, in a recent report the lower force on the guest molecule at the window has not been found [29]. More studies are required to understand the origin of the observed diffusivity maximum.

The activation energy for diffusion can be obtained from an Arrhenius plot of  $\log(D)$  vs.  $1/T$ , where  $T$  is the temperature and  $D$  is the diffusivity. Variation of activation energy as a function of the guest diameter has been plotted in **Figure 6** [30]. It is seen that the activation energy is higher for the linear regime than for the anomalous regime guests. It is also seen that activation energy is maximum for the size with minimum diffusivity and minimum for the guest size in the AR with maximum diffusivity.

The observed behavior has been termed the levitation effect (LE) as its origin is in the dispersion forces, which cancel each other leading to reduced forces on the guest molecule with maximum diffusivity. Unlike diffusion of p-xylene and o- and m-xylenes whose diffusivities are controlled by the steric repulsion and therefore only p-xylene manages to diffuse, here the diffusivities are controlled by the dispersion forces, which are always attractive in nature.

Arrhenius plots for two sizes, namely, 4.96 Å and 6.0 Å are shown in **Figure 7** [28]. The smaller sized guest atom has a higher slope and activation energy than the larger sized guest atom. The activation energies for the smaller and larger sized guest atoms are respectively 5.89 kJ/mol and 3.26 kJ/mol.

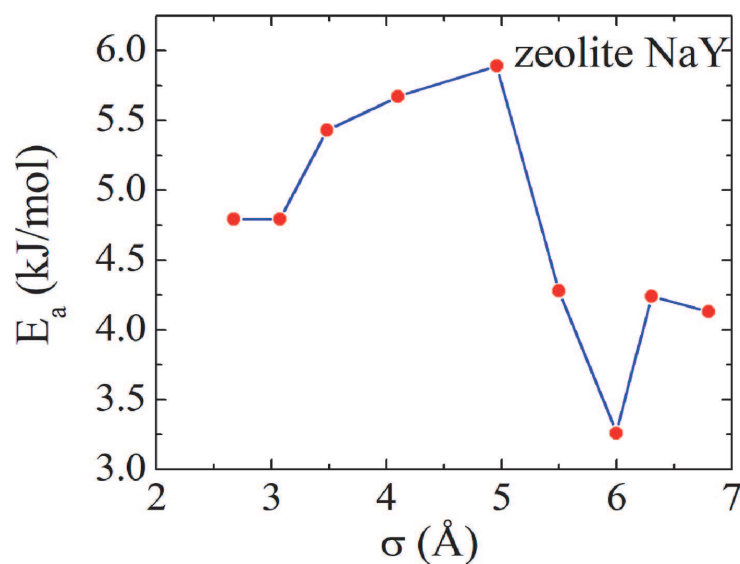


**Figure 6.**

Variation of activation energy  $E_a$  as a function of vdw radius of guests,  $\sigma$  in zeolite NaY.

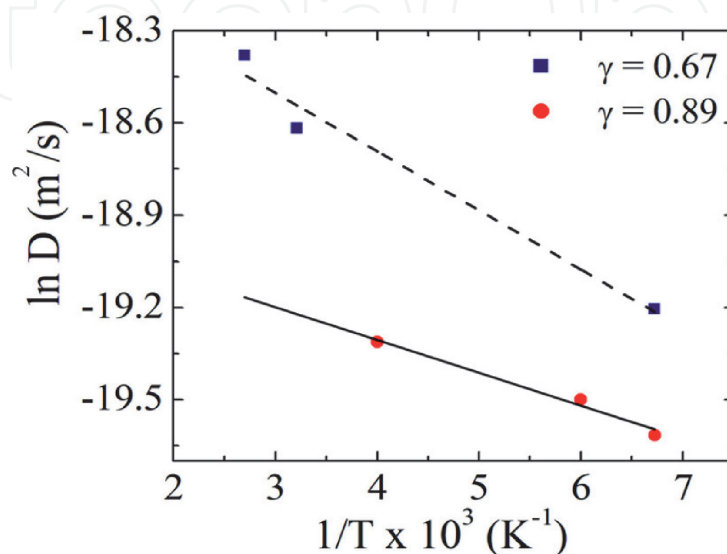


**Figure 7.**

Arrhenius plot of  $\ln D$  for two different values of  $\gamma = 0.67$  and  $0.89$  in zeolite NaY.

## 2.1 Effect of temperature on the levitation effect

The diffusivity maximum or the levitation effect is a consequence of the existence of dispersion forces. If the attractive part of the guest-zeolite interaction is switched off, then the diffusivity maximum disappears. This is shown in **Figure 8** [28]. Temperature plays an important role in the behavior of the diffusion coefficient as a function of the guest diameter.

At very higher temperatures the diffusivity maximum altogether disappears. This can be seen in **Figure 9** [31]. What determines the temperature at which the diffusivity maximum will vanish? It is the strength of interaction between the guest and the zeolite. At relatively higher temperatures when  $k_B T \gg U_{gz}$  the diffusivity maximum vanishes and only a monotonic dependence on guest diameter is seen.

At low temperatures, the diffusivity maximum is very pronounced with the diffusivity of the guest of 6.0 Å (in zeolite Y) showing several orders of magnitude higher value than the diffusivity of the 4.96 Å guest. This is shown in **Figure 9** [31].

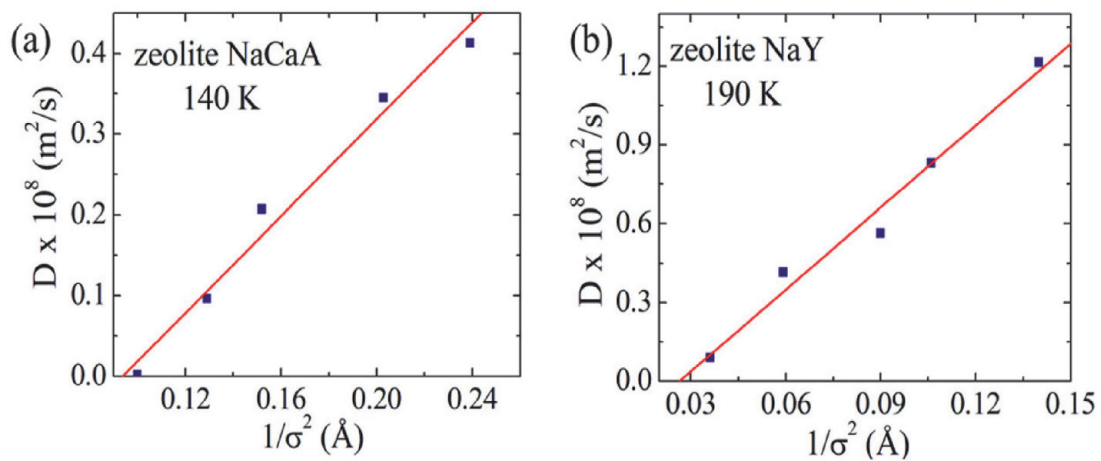


**Figure 8.** Variation of diffusion coefficient  $D$  as a function of  $1/\sigma^2$  in (a) zeolite NaCaA and (b) zeolite NaY, where  $\sigma$  is the van der Waals diameter of guest atoms. This plot is obtained without taking into account the dispersion force between guest and host atoms during molecular dynamics simulation. This clearly shows that the levitation effect is a resulting phenomenon from dispersion force of attraction.

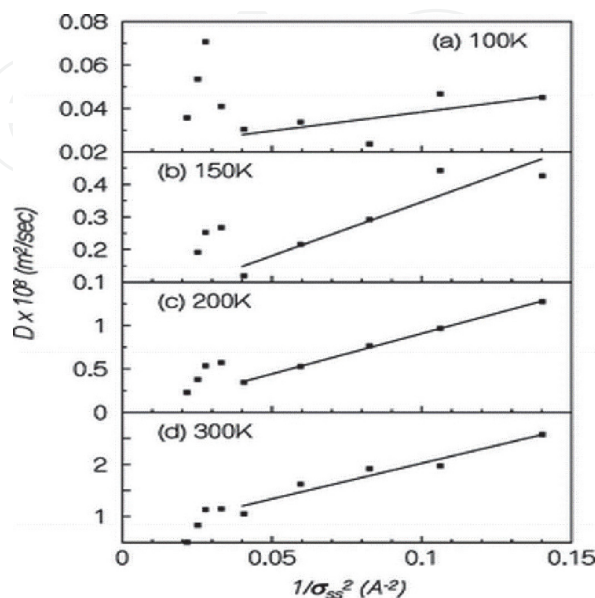


**Figure 9.** Diffusion coefficient  $D$  as a function of  $1/\sigma^2$  in zeolite NaY at different temperatures. It is depicted that the maxima in diffusivity disappear with increase in temperature.

At very low temperatures, the diffusivity maximum is seen to be very pronounced [32]. This can be seen from **Figure 10**. The difference between the anomalous regime guest and the linear regime guest is now several orders of magnitude. This can not be easily utilized in the practice because of the low diffusivities of both the species.

Smit and coworkers have reported a study on carbon nanotubes (CNTs). They investigated diffusion of methane in CNTs of different diameters. They found that the diffusion coefficient is maximum in the CNTs with similar diameter as the methane. They also carried out a simulation at higher temperatures when the height of the diffusivity maximum decreased and eventually disappeared similar to the disappearance of the maximum in the zeolite.

Many of these simulations have been carried out with the zeolite framework fixed. Will the diffusivity maximum persist when the framework is flexible? For this, simulations with flexible framework were carried out and the results are shown in **Figure 11** [33]. As can be seen the diffusivity maximum persists in spite of the framework flexibility. The height of the maximum is marginally lower and slightly shifted to lower values of guest diameter.

Kar and Chakravarty reported instantaneous normal mode analysis of guest of different diameters to understand the levitation effect. They could reproduce the velocity autocorrelation functions of various guest molecules in zeolite NaY [34]. Bhattacharyya and coworkers have carried out a mode coupling analysis of the levitation effect [35].

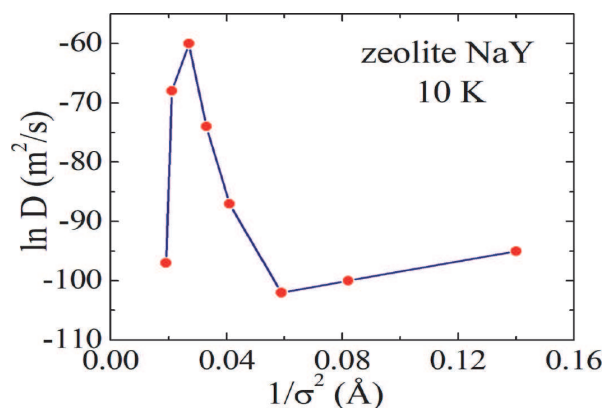


**Figure 10.** Diffusion coefficient  $D$  as a function of  $1/\sigma^2$  in zeolite NaY at 10 K. The diffusivity enhances to 17 orders in natural logarithmic scale.

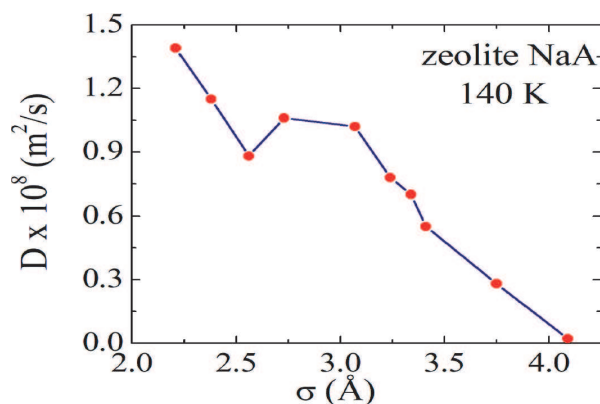


**Figure 11.** Plot of diffusion coefficient  $D$  as a function of  $\sigma$  in flexible zeolite NaA at 140 K.

## 2.2 Studies on real molecular systems

Until now simulations have been on monatomic guest species diffusion in the pores of the zeolites. These guest molecules are not of interest in real laboratory or industry. Simulations were therefore carried out on hydrocarbons molecules within zeolites to see if the observed anomalous diffusion can be observed in these real hydrocarbons. Simulations were carried out on pentane isomers: *n*-pentane, isopentane, and neopentane. These are anisotropic molecules. Hence, the dimensions of these molecules along different directions are different. For *n*-pentane the direction that is relevant is the dimension of the molecule perpendicular to its long axis. The relevant dimension for the other molecule, which is isopentane, is also the dimension perpendicular to its long axis. For neopentane, which is tetrahedral in shape, the molecular diameter is the relevant dimension. There have been attempts to compute and list the various dimensions of hydrocarbon and other molecules [36]. These can be helpful in computing the  $\gamma$  values for various guest-zeolite systems.

Simulations of pentane isomers, *n*-pentane, and isopentane in AlPO-5, which has one-dimensional channels, have been reported [37]. These studies show that isopentane has a higher diffusivity as compared to *n*-pentane. Thus, anomalous diffusion is seen even in AlPO-5. The diffusivities obtained are  $2.7 \times 10^{-8} \text{ m}^2/\text{s}$  and  $3.33 \times 10^{-8} \text{ m}^2/\text{s}$  for *n*-pentane and isopentane respectively at 300 K. The potential parameters employed in this study were the unified potential parameters of Jorgensen [38]. The potential parameters are very similar to the OPLS parameters later proposed by Jorgensen. Masses of the isomers are identical and therefore the difference in the diffusivity arises from the difference in  $\gamma$ . For AlPO-5, it is seen that the  $\gamma$  values are 0.71 and 0.88 respectively for *n*-pentane and isopentane. The value of  $\gamma$ , which separates linear and anomalous regime, is around 0.75. This boundary will vary and depends on the zeolite but as a rule of thumb, a value of 0.75 may be used. The value of 0.71 lies in the linear regime while 0.88 lies in the anomalous regime. Thus, *n*-pentane with lower  $\gamma$  has a lower diffusivity, which is what one expects.

## 2.3 Experimental verification of the diffusivity maximum

The diffusivity of a species changes with its mass as well as other parameters such as size, temperature, etc. In simulations, the diameter of the diffusing species were changed without changing its mass. Ideally, an experimental verification of the levitation effect should do the same, that is change the diameter without changing the mass. But in real laboratory this appears almost impossible. However, Dr. S.G.T. Bhat during one of our discussions mentioned that this indeed is possible. He suggested use of isomers of a hydrocarbon all of which will have the same mass but differ in their cross-sectional diameter [39]. The choice of the experiments was also crucially important. Different techniques of measuring the diffusivity such as uptake, NMR, ZLC, or QENS yield different values of for the diffusivity of the same species. Kärger and coworkers have investigated the reasons for this [40, 41]. They have suggested that this is due to the difference in the sampling time and length scales. As MD sample over picoseconds to nanoseconds, a technique which samples for similar time scale would be ideal. As QENS samples over the same period, we choose to carry experiments with this technique. We chose zeolite NaY with three isomers of pentane, namely, *n*-pentane, isopentane, and neopentane. The diameters of these were calculated from their geometry and Lennard-Jones interaction parameters. Knowing the 12-ring window diameter of faujasite, we computed the levitation parameters  $\gamma$  for these isomers, which are 0.71, 0.86, and 0.96 for

*n*-pentane, isopentane, and neopentane. The experimental QENS spectra are given in **Figure 12** [42, 43]. Also shown are the variation in half width at half maximum (HWHM) as a function of  $Q^2$ . From the broadening of the spectra as a function of  $Q^2$ , one obtains the diffusivity. The HWHM increases fastest for neopentane, followed by isopentane and last is *n*-pentane. These suggest that neopentane has the highest diffusivity, followed by isopentane and *n*-pentane in that order.

## 2.4 Hexane isomers in faujasite

Diffusion of hexane isomers in zeolite NaY was carried out with the help of MD technique. Linear hydrocarbons *n*-hexane (*n*C6), singly branched isomers 2-methyl pentane (2MP) and 3-methyl pentane (3MP) as well as the doubly branched isomers 2,2-dimethyl butane (22DMB) and 2,3-dimethyl butane (23DMB) were studied [44]. The calculated adsorption energies from MD of different isomers of hexane are listed in **Table 1**.

There is little difference in the adsorption energies of the isomers. Hence, it is difficult to separate the isomers from each other using a method based on adsorption. Instead, a kinetic-based approach might be helpful for separating the mixtures consisting of hexane isomers. In **Figure 13** the mean squared displacements of the isomers are shown for 2.25 ns. The lines are all straight suggesting good statistics [44]. The diffusivities of the isomers at these temperatures are listed in **Table 2**.

The cross-sectional diameter of the isomers can be computed from the geometry of the isomers. These are listed in **Table 3** along with the  $\gamma$  values for the isomers [44]. As can be seen except for *n*-hexane other isomers are all in the anomalous regime.

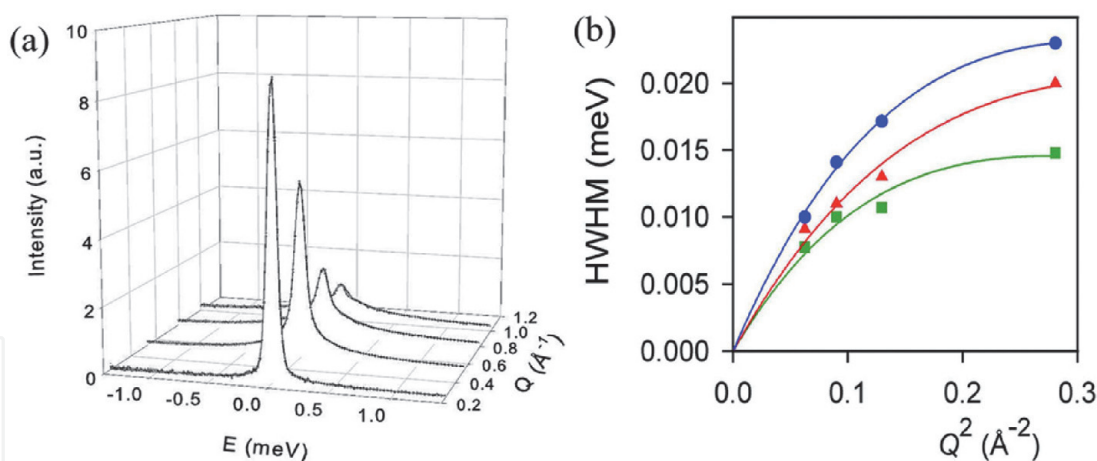


**Figure 12.**

(a) Spectra of QENS obtained for neopentane at 300 K for different values of the wave vector transfer  $Q$  and (b) HWHM vs.  $Q^2$  corresponding to the translational motion of the pentane isomers in zeolite NaY at 300 K, neopentane (triangles), isopentane (squares), and *n*-pentane (circles).

Isomer	$E_{ads}$ (kJ/mol)
<i>n</i> -Hexane	-46.7
2-Methylpentane	-45.9
3-Methylpentane	-46.4
2,3-Dimethylbutane	-45.9
2,2-Dimethylbutane	-45.8

**Table 1.**

Adsorption energies  $E_{ads}$  of hexane isomers in zeolite NaY.

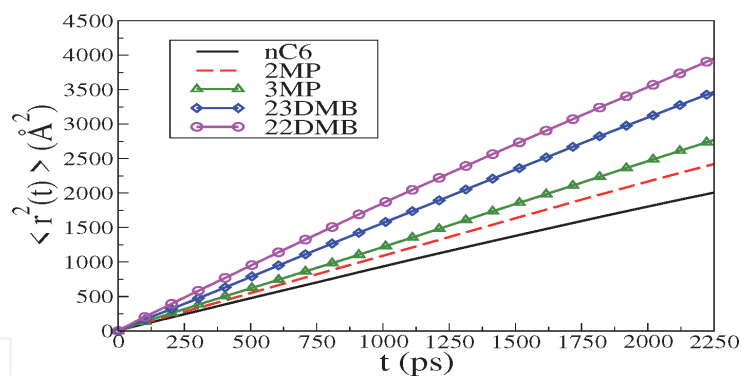


**Figure 13.**  
 Mean square displacement of hexane isomers in zeolite NaY at 250 K.

Isomer	250 K	300 K	330 K	350 K	400 K
<i>n</i> -Hexane	1.43(0.24)	3.59(0.35)	5.07(0.40)	7.27(0.61)	10.47(0.50)
2-Methylpentane	1.79(0.09)	3.17(0.21)	4.58(0.50)	6.44(0.55)	9.78(0.57)
3-Methylpentane	2.04(0.12)	3.92(0.24)	5.49(0.42)	6.23(0.44)	10.44(0.66)
2,3-Dimethylbutane	2.57(0.19)	4.68(0.32)	6.63(0.30)	7.26(0.61)	10.60(0.8)
2,2-Dimethylbutane	2.91(0.38)	5.67(0.29)	7.39(0.39)	7.75(0.46)	11.43(0.38)

**Table 2.**  
 Diffusion coefficients of hexane isomers in zeolite Y.

Isomer	$\sigma_{\perp}$ (Å)	$\gamma$
<i>n</i> -Hexane	6.905	0.69
2-Methylpentane	8.09	0.80
3-Methylpentane	9.55	0.95
2,3-Dimethylbutane	9.96	0.98
2,2-Dimethylbutane	10.31	1.02

**Table 3.**  
 Molecular diameter perpendicular to the long axis ( $\sigma_{\perp}$ ) and the levitation parameter ( $\gamma$ ) values of all hexane isomers, when adsorbed in zeolite NaY.

From the Arrhenius plots of diffusivity (see **Figure 14**), we have obtained the activation energies [44]. These are listed in **Table 4** [44]. It is seen that the activation energies of *n*-hexane is the highest at 11.2 kJ/mol. 2MP has an activation energy

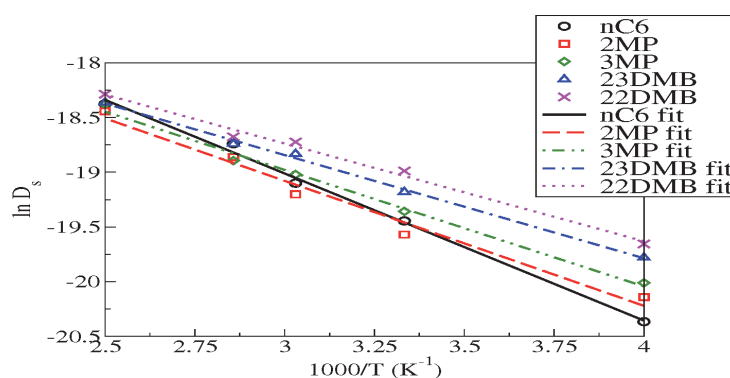


**Figure 14.**  
 Arrhenius plot of various hexane isomers in zeolite NaY.

Isomer	$E_a$ (kJ/mol)
<i>n</i> -Hexane	11.2
2-Methylpentane	9.5
3-Methylpentane	8.8
2,3-Dimethylbutane	7.8
2,2-Dimethylbutane	7.4

**Table 4.**  
Activation energies  $E_a$  of hexane isomers in zeolite NaY.

of 9.5 kJ/mol followed by 3MP (8.8 kJ/mol). The doubly branched isomers 23DMB (7.8 kJ/mol) and 22DMB (7.4 kJ/mol) have the lowest activation energy. These trends in the activation energies are according to what one expects based on the levitation effect.

The potential energy landscape of the various isomers as they diffuse during the passage through the 12-ring window of zeolite NaY is given in **Figure 15** [44]. It is seen that *n*-hexane alone has a maximum in the potential energy at the 12-ring window. 23DMB has a small maximum but overall it is a negative barrier in the vicinity of the window.

#### 2.4.1 Kinetic-based separation of hexane isomers

Arrhenius plots of diffusivities for various isomers cross each other at some temperature. Consider two isomers. They cross at some temperature referred to as the inversion temperature. Above the temperature if one isomer has a higher diffusivity, the same isomer below the inversion temperature will have the lower diffusivity among the two isomers. The Arrhenius plots of various isomers are plotted in **Figure 16** [44]. Various pairs of isomers cross each other at different temperatures. These are listed in **Table 5** [44]. Thus, from the table it is evident that pairs 2MP/*n*-hexane have an inversion temperature of 300 K. As *n*-hexane has higher activation energy of the two, at  $T < 300$  K, 2MP will exit from a column first and then *n*-hexane. At  $T > 300$  K, *n*-hexane will have higher diffusivity and exit from the column first, followed by 2MP. The order of exit of the various isomers from a zeolite single crystal is seen to be different at different temperatures. There are in all 11 regions, which correspond to different order in which the isomers will exit. The order of diffusivities or the order of exit of the various isomers is listed in **Table 6** [44]. As the temperature is increased from below 300 K upto 1172 K, the order of diffusivities of various isomers is given.

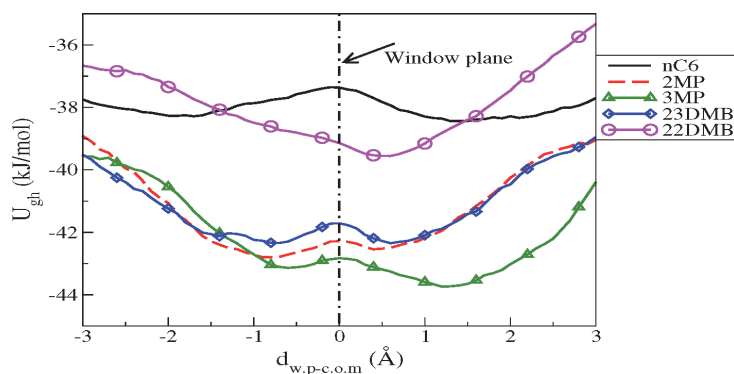


**Figure 15.**  
Potential energy landscape for hexane isomers in zeolite NaY at 250 K. these plots are obtained by averaging over all cage-to-cage jumps.

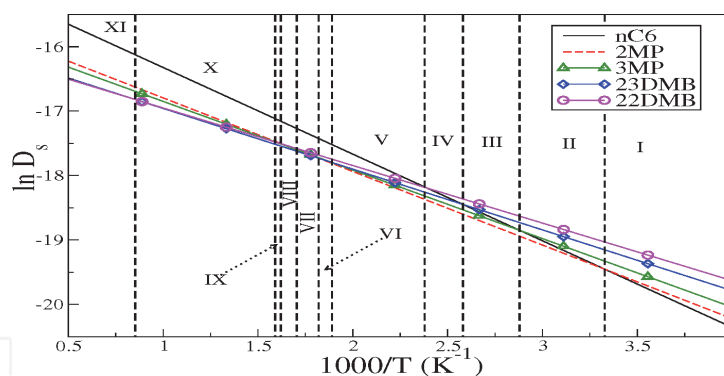


**Figure 16.**  
 Change of order of diffusivity for various hexane isomers in zeolite NaY.

Molecules inverted	$T_{inv}$ (K)
2MP/nC6	300
MP/nC6	347
DMB/nC6	387
DMB/nC6	418
DMB/3MP	528
DMB/2MP	549
MP/2MP	586
DMB/2MP	613
DMB/3MP	627
DMB/23DMB	1172

**Table 5.**  
 Inversion temperatures for diffusivities ( $T_{inv}$ ) of hexane isomers inside zeolite NaY.

Region	Temp range (K)	Order of diffusivities
I	$T < 300$	nC6 < 2MP < 3MP < 23DMB < 22DMB
II	300,347	2MP < nC6 < 3MP < 23DMB < 22DMB
III	347,387	2MP < 3MP < nC6 < 23DMB < 22DMB
IV	387,418	2MP < 3MP < 23DMB < nC6 < 22DMB
V	418,528	2MP < 3MP < 23DMB < 22DMB < nC6
VI	528,549	2MP < 23DMB < 3MP < 22DMB < nC6
VII	549,586	23DMB < 2MP < 3MP < 22DMB < nC6
VIII	586,613	23DMB < 3MP < 2MP < 22DMB < nC6
IX	613,627	23DMB < 3MP < 22DMB < 2MP < nC6
X	6,271,172	23DMB < 22DMB < 3MP < 2MP < nC6
XI	$T > 1172$	22DMB < 23DMB < 3MP < 2MP < nC6

**Table 6.**  
 Different regions according to order of diffusivities of hexane isomers in zeolite NaY.

## 2.5 End-to-end length of *n*-hexane during diffusion

An interesting observation from the study was the variation of end-to-end length,  $L_{e-e}$  of *n*-hexane during diffusion. The  $L_{e-e}$  was computed at various temperatures for *n*-hexane. It showed that there is a decrease in the end-to-end length of *n*-hexane as the temperature increases. A plot of average  $L_{e-e}$  as a function of the temperature is shown in **Figure 17** [44]. The distribution of the  $L_{e-e}$  has also been computed for various temperatures and these are shown in **Figure 18** [44]. As can be seen at higher temperatures the distribution has a higher probability for smaller values of  $L_{e-e}$ , between 3 and 5 Å and less probability for higher values (5–6.4 Å) of  $L_{e-e}$ . This is what leads to a decrease in average  $L_{e-e}$  with temperature. These suggest that *n*-hexane curls up at higher temperatures and has a higher population of gauche conformers. In order to check if this was true, we have obtained the number of gauche conformer population and these are listed in **Table 7**.

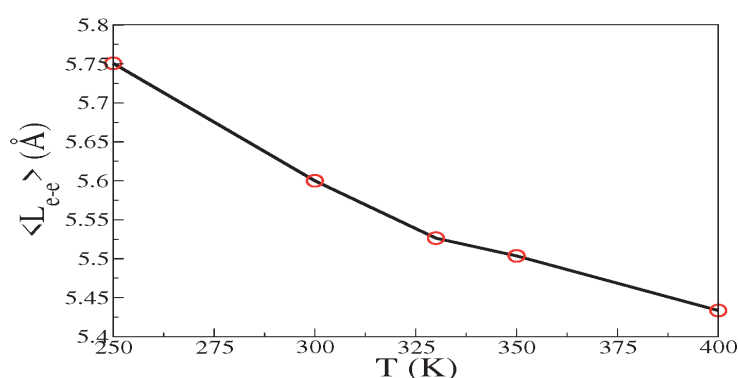


**Figure 17.**  
Variation of end-to-end length of *n*-hexane in zeolite NaY as a function of temperature.

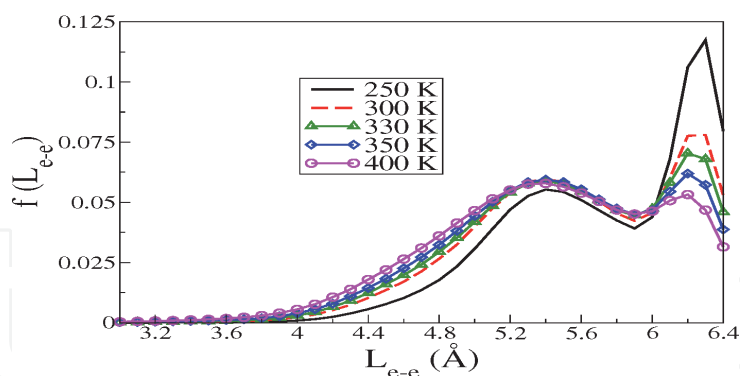


**Figure 18.**  
Distribution of end-to-end length *n*-hexane in zeolite NaY at various temperatures.

Temp (K)	$\phi_1$	$\phi_2$	$\phi_3$
250	24.9	19.0	24.7
300	29.5	23.8	29.4
330	32.3	26.4	32.5
350	34.3	28.2	34.3
400	36.5	30.4	36.6

**Table 7.**  
% gauche conformations for each dihedral angle of *n*C6 inside zeolite NaY at various temperatures.

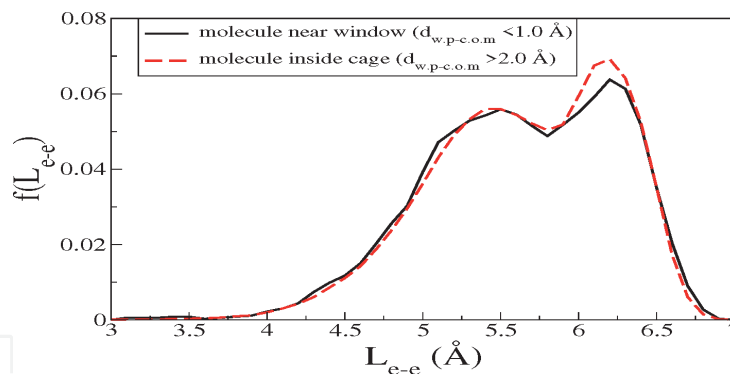


**Figure 19.**  
Variation of the distribution of end-to-end length of *n*C6 in zeolite NaY.

The distribution of end-to-end length of *n*-hexane is shown in **Figure 19** for two specific situations: (i) when the center of mass of *n*-hexane is close to the 12-ring window (within  $\pm 1.0$  Å) and (ii) when the center of mass is greater than 2 Å from the window plane [44]. As can be seen, the probability for smaller values of  $L_{e-e}$  is higher when the molecule of *n*-hexane is closer to the window. Thus, it appears that the *n*-hexane curls up trying to increase its cross-sectional diameter while passing through the 12-ring window. This leads to a slightly lower value of energetic barrier for *n*-hexane when it curls up.

## 2.6 Separation using levitation effect

Using the levitation effect, separation of molecular mixtures can be realized. This approach differs from the usual approach toward separation. In the usual approach separation is achieved because the smaller sized molecules generally diffuse faster as compared to larger sized guest molecules. Or alternately, certain molecules enter the pores while bigger sized molecules do not even enter the pore network. In this case only those which enter the pores are able to pass through the column of the zeolite while others are unable to pass through leading to good separation.

Consider now a binary mixtures in which both the components are able to enter the pore network. When we use the levitation effect, both mixtures will diffuse but here the larger sized guest will diffuse faster provided the bottleneck of the zeolite has a diameter that is comparable to the diameter of the larger sized guest molecule. The smaller diameter guest molecule will diffuse slower and this leads to separation of the components.

In all these separations, however, one thing that is common is that both the components (in the case of a binary mixture) will diffuse in the same direction. This leads at best to a reasonable degree of separation. However, much higher degree of separation can be achieved if the two components move in opposite directions. We have devised a novel approach to separation in which the two components move in opposite directions [45]. In this approach, the fact that the guest in AR and the LR regimes have out-of-phase potential energy landscape is utilized. This is shown in **Figure 20** [45]. In addition, a hot zone is placed to the left of the 12-ring window in the system consisting of zeolite A with argon (of AR) and neon (of LR). The hot zone drives argon toward the left and the neon toward to right. The result is a very high degree of separation. This has been demonstrated through nonequilibrium Monte Carlo simulations with inhomogeneous temperature [45]. In **Figure 21** a plot of the separation factor as a function of Monte Carlo steps is shown. Normally separation factors that are achieved are of the order of 2000–4000. But here we see that separation factors of the order of  $>10^{8-10}$  can be realized.

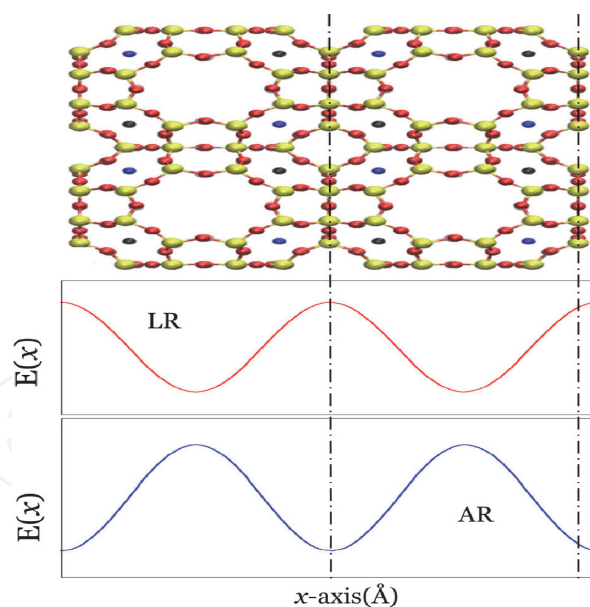


**Figure 20.** Schematic of potential energy landscapes of AR (BLUE) and LR (RED) particles are shown below the unit cell crystal structure of zeolite NaCaA. The black dotted lines are the window planes of the zeolite.

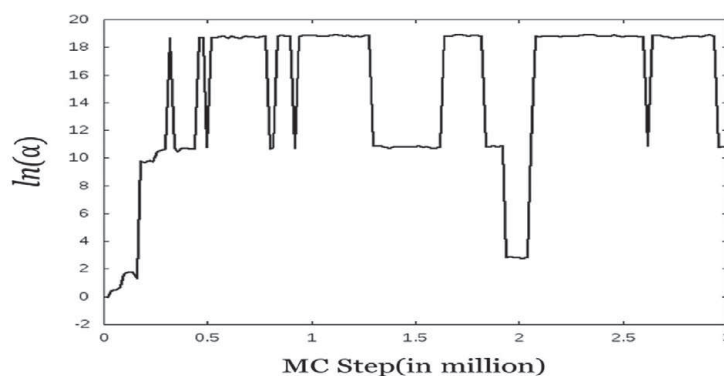


**Figure 21.** Evolution of separation factor with Monte Carlo steps. This shows that AR particles can be fully separated from LR particles using this separation technique.

### 3. Conclusions

The surprising anomaly in the diffusivity of a guest diffusing within the confined regions of a zeolite or a CNT or any other porous solid has many uses. It also explains the observed increase in ionic conductivity as a function of ionic radius on going from  $\text{Li}^+$  to  $\text{Na}^+$  to  $\text{K}^+$  and  $\text{Rb}^+$  and  $\text{Cs}^+$  [46]. Levitation effect was first observed in the experiments by Kemball and later Derouane showed its existence through theory [47–49]. It can be used in the separation of molecular mixtures as well as in separations of very high degree. Levitation effect can be better put into practice with single crystals and nano devices.

### Acknowledgements

The authors wish to acknowledge support from Department of Science and Technology, New Delhi and computational facilities from Thematic Unit of Excellence for Computational Materials Science established with support from Nano Mission, DST, New Delhi.

IntechOpen

IntechOpen

### **Author details**

Shubhadeep Nag and Yashonath Subramanian\*  
Solid State and Structural Chemistry Unit, Indian Institute of Science, Bengaluru,  
India

\*Address all correspondence to: [yashonath@iisc.ac.in](mailto:yashonath@iisc.ac.in)

### **IntechOpen**

---

© 2020 The Author(s). Licensee IntechOpen. This chapter is distributed under the terms of the Creative Commons Attribution License (<http://creativecommons.org/licenses/by/3.0>), which permits unrestricted use, distribution, and reproduction in any medium, provided the original work is properly cited. 

## References

- [1] Boronat M, Corma A. What is measured when measuring acidity in zeolites with probe molecules? *ACS Catalysis*. 2019;**9**(2):1539-1548
- [2] Moliner M, Corma A. From metal-supported oxides to well-defined metal site zeolites: The next generation of passive nox adsorbers for low-temperature control of emissions from diesel engines. *Reaction Chemistry & Engineering*. 2019;**4**:223-234
- [3] Li C, Moliner M, Corma A. Building zeolites from precrystallized units: Nanoscale architecture. *Angewandte Chemie International Edition*. 2018; **57**(47):15330-15353
- [4] Bereciartua PJ, Cantín Á, Corma A, Jordá JL, Palomino M, Rey F, et al. Control of zeolite framework flexibility and pore topology for separation of ethane and ethylene. *Science*. 2017; **358**(6366):1068-1071
- [5] Sastre G, Kärger J, Ruthven DM. Diffusion path reversibility confirms symmetry of surface barriers. *The Journal of Physical Chemistry C*. 2019; **123**(32):19596-19601
- [6] Toda J, Sastre G. Diffusion of trimethylbenzenes, toluene, and xylenes in uwy zeolite as a catalyst for transalkylation of trimethylbenzenes with toluene. *The Journal of Physical Chemistry C*. 2018;**122**(14):7885-7897
- [7] Zachariou A, Hawkins A, Lennon D, Parker SF, Suwardiyanto SK, Matam CRA, et al. Investigation of zsm-5 catalysts for dimethylether conversion using inelastic neutron scattering. *Applied Catalysis A: General*. 2019;**569**:1-7
- [8] Caro J, Kärger J. From computer design to gas separation. *Nature Materials*
- [9] Kumar P, Kim DW, Rangnekar N, Xu H, Fetisov EO, Ghosh S, et al. One-dimensional intergrowths in two-dimensional zeolite nanosheets and their effect on ultra-selective transport. *Nature Materials*. 2020;**19**:443-449
- [10] Quesne MG, Silveri F, de Leeuw NH, Catlow CRA. Advances in sustainable catalysis: A computational perspective. *Frontiers in Chemistry*. 2019;**7**:182
- [11] Kang JH, Alshafei FH, Zones SI, Davis ME. Cage-defining ring: A molecular sieve structural indicator for light olefin product distribution from the methanol-to-olefins reaction. *ACS Catalysis*. 2019;**9**(7):6012-6019
- [12] Dusselier M, Davis ME. Small-pore zeolites: Synthesis and catalysis. *Chemical Reviews*. 2018;**118**(11):5265-5329
- [13] Davis ME. A thirty-year journey to the creation of the first enantiomerically enriched molecular sieve. *ACS Catalysis*. 2018;**8**(11):10082-10088
- [14] Barrer RM. *Hydrothermal Chemistry of Zeolites*. London: Academic Press; 1982
- [15] Kärger J, Ruthven DM. *Diffusion in Zeolites and Other Microporous Solids*. New York, USA: John Wiley and Sons Inc.; 1992
- [16] Dong J, Lin YS, Liu W. Multicomponent hydrogen/hydrocarbon separation by mfi-type zeolite membranes. *AIChE Journal*. 2000;**46**(10):1957-1966
- [17] Arruebo M, Falconer JL, Noble RD. Separation of binary c5 and c6 hydrocarbon mixtures through mfi zeolite membranes. *Journal of Membrane Science*. 2006;**269**(1):171-176
- [18] Seader JD, Henley EJ. *Separation Process Principles*. 1st ed. New York, USA: John Wiley and Sons Inc.; 1998

- [19] Colella C. Ion exchange equilibria in zeolite minerals. *Mineralium Deposita*. 1996;**31**(6):554-562
- [20] Loiola A, Andrade J, Sasaki J, da Silva L. Structural analysis of zeolite naa synthesized by a cost-effective hydrothermal method using kaolin and its use as water softener. *Journal of Colloid and Interface Science*. 2012; **367**(1):34-39
- [21] Smit B, Maesen TLM. Molecular simulations of zeolites: Adsorption, diffusion, and shape selectivity. *Chemical Reviews*. 2008;**108**(10): 4125-4184
- [22] Tarditi AM, Horowitz GI, Lombardo EA. Xylene isomerization in a zsm-5/ss membrane reactor. *Catalysis Letters*. 2008;**123**(1):7-15
- [23] Young L, Butter S, Kaeding W. Shape selective reactions with zeolite catalysts: Iii. Selectivity in xylene isomerization, toluene-methanol alkylation, and toluene disproportionation over zsm-5 zeolite catalysts. *Journal of Catalysis*. 1982;**76**(2): 418-432
- [24] Dubbeldam D, Calero S, Maesen TLM, Smit B. Understanding the window effect in zeolite catalysis. *Angewandte Chemie International Edition*. 2003;**42**(31):3624-3626
- [25] Kärger J, Petzold M, Pfeifer H, Ernst S, Weitkamp J. Single-file diffusion and reaction in zeolites. *Journal of Catalysis*. 1992;**136**(2): 283-299
- [26] Yashonath S, Ghorai PK. Diffusion in nanoporous phases: Size dependence and levitation effect. *The Journal of Physical Chemistry B*. 2008;**112**(3): 665-686
- [27] Yashonath S, Santikary P. Influence of non-geometrical factors on intracrystalline diffusion. *Molecular Physics*. 1993;**78**(1):1-6
- [28] Yashonath S, Santikary P. Diffusion of sorbates in zeolites y and a: Novel dependence on sorbate size and strength of sorbate-zeolite interaction. *The Journal of Physical Chemistry*. 1994; **98**(25):6368-6376
- [29] Sharma A, Ghorai PK. Effect of force and location of bottleneck for particle moving through window under encapsulation. *Journal of Chemical Science*. 2017;**129**(8):1293-1300
- [30] Rajappa C, Yashonath S. Levitation effect and its relationship with the underlying potential energy landscape. *The Journal of Chemical Physics*. 1999; **110**(12):5960-5968
- [31] Yashonath S, Rajappa C. Temperature dependence of the levitation effect implications for separation of multicomponent mixtures. *Faraday Discussions*. 1997;**106**:105-118
- [32] Ghorai PK, Yashonath S. Diffusion anomaly at low temperatures in confined systems from the rare events method. *The Journal of Physical Chemistry B*. 2004;**108**(22):7098-7101
- [33] Santikary P, Yashonath S. Dynamics of zeolite cage and its effect on the diffusion properties of sorbate: Persistence of diffusion anomaly in naa zeolite. *The Journal of Physical Chemistry*. 1994;**98**(37):9252-9259
- [34] Kar S, Chakravarty C. Instantaneous normal mode analysis of the levitation effect in zeolites. *The Journal of Physical Chemistry B*. 2000;**104**(4):709-715
- [35] Nandi MK, Banerjee A, Bhattacharyya SM. Non-monotonic size dependence of diffusion and levitation effect: A mode-coupling theory analysis. *The Journal of Chemical Physics*. 2013; **138**(12):124505
- [36] Federico J-C, Laredo GC. Molecular size evaluation of linear and branched paraffins from the gasoline pool by dft

- quantum chemical calculations. *Fuel*. 2004;**83**:2183-2188
- [37] Bhide SY, Kumar AVA, Yashonath S. Diffusion of hydrocarbons in confined media: Translational and rotational motion. *Journal of Chemical Sciences*. 2001;**113**(5):559-577
- [38] Jorgensen WL, Madura JD, Swenson CJ. Optimized intermolecular potential functions for liquid hydrocarbons. *Journal of the American Chemical Society*. 1984;**106**(22): 6638-6646
- [39] Personal communication with Dr. S.G. Thirumaleshwara Bhat.
- [40] Kärger J, Ruthven DM. On the comparison between macroscopic and n.m.r. measurements of intracrystalline diffusion in zeolites. *Zeolites*. 1989;**9**(4): 267-281
- [41] Kärger J, Ruthven DM. Diffusion in nanoporous materials: Fundamental principles, insights and challenges. *New Journal of Chemistry*. 2016;**40**: 4027-4048
- [42] Borah BJ, Jobic H, Yashonath S. Levitation effect in zeolites: Quasielastic neutron scattering and molecular dynamics study of pentane isomers in zeolite nay. *The Journal of Chemical Physics*. 2010;**132**(14):144507
- [43] Jobic H, Borah BJ, Yashonath S. Neutron scattering and molecular dynamics evidence for levitation effect in nanopores. *The Journal of Physical Chemistry B*. 2009;**113**(38):12635-12638
- [44] Thomas AM, Subramanian Y. Hexane isomers in faujasite: Anomalous diffusion and kinetic separation. *The Journal of Physical Chemistry C*. 2017; **121**(27):14745-14756
- [45] Anil Kumar AV, Yashonath S, Ananthakrishna G. Separation of mixtures at nano length scales: Blow torch and levitation effect. *The Journal of Physical Chemistry B*. 2006;**110**(8): 3835-3840
- [46] Ghorai PK, Yashonath S. Evidence in support of levitation effect as the reason for size dependence of ionic conductivity in water: A molecular dynamics simulation. *The Journal of Physical Chemistry B*. 2006;**110**(24): 12179-12190
- [47] Kemball C. Entropy of adsorption. *Advances in Catalysis*. 1950;**2**:233-250
- [48] Derouane EG. The energetics of sorption by molecular sieves: Surface curvature effects. *Chemical Physics Letters*. 1987;**142**(3):200-204
- [49] Derouane EG, Andre J-M, Lucas AA. Surface curvature effects in physisorption and catalysis by microporous solids and molecular sieves. *Journal of Catalysis*. 1988;**110**(1): 58-73